

Synthesis, Characterization and Crystal Structure of the First Trinuclear MFe_2 ($M = Cu$ and Ni) Complexes Based on Nitroprusside

ZHOU, Bei-Chuan^a(周北川) KOU, Hui-Zhong^{* a}(寇会忠) LI, Yong^a(李勇)
XIONG, Ming^b(熊明) WANG, Ru-Ji^a(王如骥)

^a Department of Chemistry, Tsinghua University, Beijing 100084, China

^b Department of Chemistry, Nankai University, Tianjin 300071, China

Three new complexes $[Ni(H_2L)]Fe(CN)_5(NO)]_2 \cdot 6H_2O$ (**1**), $[Ni(H_2L)]Fe(CN)_5(NO)] \cdot 4H_2O$ (**2**) and $[Cu(H_2L)]Fe(CN)_5(NO)] \cdot 4H_2O$ (**3**) ($L = 3,10$ -bis(2-aminoethyl)-1,3,5,8,10,12-hexaazacyclotetradecane) are prepared and characterized by IR, elemental analyses and single-crystal X-ray analyses, indicating that they are the first examples of trinuclear nitroprusside-bridged MFe_2 ($M = Cu$ and Ni) complexes. In the three complexes, the central metal atoms (M) are all six-coordinated by the nitrogen atoms from the macrocyclic ligand and two cyano-bridges at the trans-positions to form distorted octahedral configurations. The axial $N-M-N$ linkage is nearly vertical to the equatorial plane defined by four coordinating N atoms of macrocyclic ligand. The $C=N-Ni$ bond angle of 172.6° in complex **1** is apparently larger than those in complexes **2** and **3** (152.57° and 136.37° , respectively). The three complexes are all connected by hydrogen bonds into 3D networks. This study shows that the cyano-bridged trinuclear species could be generated via the control of the charge of the building blocks.

Keywords copper complex, nickel complex, nitroprusside, cyano bridge, crystal structure

Introduction

Since 1848, when Playfair published the first paper related to nitroprussides,¹ the transition metal pentacyanonitrosylmetallate hydrates have been widely studied because of their important roles in molecular sieves, cation exchangers, electron scavengers and radionuclide sorbents.²⁻⁴ The nitroprussides, regardless of the cationic metal, are currently employed as reversible inhibitors of a group of enzymes known as superoxide dismutases.⁵

Recently, using $[Fe(CN)_5(NO)]^{2-}$ as a building block, some nitroprusside-bridged polymeric complexes have been prepared and magnetic studies showed that the nitroprusside anion transmits a very weak antiferromagnetic interaction.⁶⁻⁸ Currently, there has been a growing interest in clarifying the structural correlation with magnetic properties of nitroprusside-bridged complexes. Tang and co-

workers reported an antiferromagnetic 2-D cyano-bridged polymeric $[Cu_2(oxpn)Fe(CN)_5(NO)]_n(H_2(oxpn)) = N, N'$ -bis(3-aminopropyl)oxamide) complex, in which a nitrogen atom of the cyano group in $[Fe(CN)_5(NO)]^{2-}$ was coordinated to one of the adjacent copper(II) ions in $[Cu_2(oxpn)]^{2+}$.⁹ The complexes $M(en)_2Fe(CN)_5(NO) \cdot nH_2O$ (where $en =$ ethylenediamine, $M = Ni(II)$ and $Cu(II)$, $n = 0$ or 1) are one-dimensional and $Cu(L)_2Fe(CN)_5(NO) \cdot nH_2O$ (where $L = 2$ -dimethylaminoethylamine,¹⁰ 1-dimethylamino-2-propylamine,¹⁰ 3,10-bis(2-hydroxyethyl)-1,3,5,8,10,12-hexaazacyclotetradecane⁸ and 1,2-diaminopropane¹¹) are cyano-bridged binuclear complexes.

In order to synthesize nitroprusside-bridged complexes with new structures,¹² we modified the four-coordinate $[ML]^{n+}$ ($M = Cu$ and Ni) cation from common divalent to tetravalent,¹³ and successfully obtained the first three trinuclear nitroprusside-bridged complexes with the formula of MFe_2 ($M = Cu$ and Ni). The complexes $[Ni(H_2L)]Fe(CN)_5(NO)]_2 \cdot 6H_2O$ (**1**), $[Ni(H_2L)]Fe(CN)_5(NO)] \cdot 4H_2O$ (**2**) and $[Cu(H_2L)]Fe(CN)_5(NO)] \cdot 4H_2O$ (**3**) ($L = 3,10$ -bis(2-aminoethyl)-1,3,5,8,10,12-hexaazacyclotetradecane) are all characterized by IR, elemental analyses and single-crystal X-ray analyses.

Results and discussion

Employing $[Ni(H_2L)]ClO_4$, $[Ni(H_2L)]Br_4$ and $[Cu(H_2L)]ClO_4$ as reagents to react with $Na_2[Fe(CN)_5(NO)] \cdot 2H_2O$ leads to three trinuclear complexes **1**, **2** and **3**, respectively. The assembly of the trinuclear molecules is probably due to the charge ratio of two building blocks. Of course, a structure consisting of one-dimensional nitroprusside-bridged alternating Ni-Fe chain with a free nitroprusside anion may be generated as a variation of the trinuclear cluster. Such a case has been seldom observed.

* E-mail: kouhz@mail.tsinghua.edu.cn; Fax: 86-10-62788765

Received March 17, 2003; revised May 12, 2003; accepted May 22, 2003.

Project supported by the National Natural Science Foundation of China (Nos. 20201008 and 50272034).

Crystal structures

The selected bond lengths and angles are listed in Table 1.

As shown in Fig. 1, the structure of complex **1** consists of a trinuclear cyano-bridged NiFe₂ molecules and lattice water molecules, in which the central Ni atom is coordinated by six N atoms to form a slightly distorted octahedron configuration. Four of the six N atoms which defined the equatorial plane are from H₂L²⁺ ligand with the average Ni—N_{equatorial} distance of 0.2066 nm and the N(7)—N(1)—N(8) angle of 85.4°. The other two N atoms at the axis are from the two cyano-bridges of two [Fe(CN)₅(NO)]²⁻ ions with the Ni—N_{axial} distance of 0.2113(6) nm. While in the one-dimensional complex Ni(en)₂Fe(CN)₅(NO),⁶ the Ni—N bond lengths (ranging from 0.2095 to 0.2099 nm) are almost the same. In complex **1**, the axial N—Ni—N linkage are linear and almost vertical to the equatorial plane which can be approved by the angles of N(7)—Ni(1)—N(1) [88.5(2)°], N(8)—Ni(1)—N(1) [90.9(2)°]. The α(1)—N(1)—N(1) angle of 172.6(6)° is nearly linear, and apparently larger than that of complex Ni(en)₂Fe(CN)₅(NO)₃ and most of the Cu—Fe

nitroprussides.⁷⁻⁹

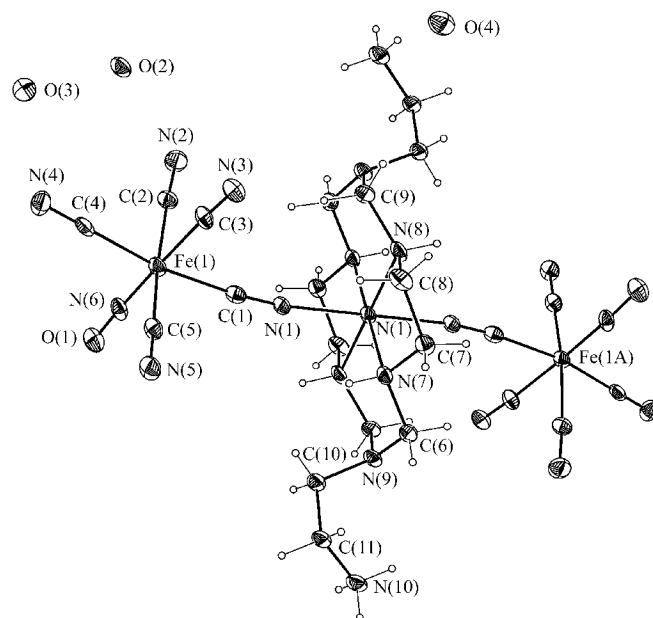


Fig. 1 ORTEP drawing of **1** with atomic numbering scheme, showing thermal ellipsoids at the 30% probability level.

Table 1 Selected bond lengths (nm) and angles (°) of **1**, **2** and **3**

	1	2	3		3
N(1)—N(1)	0.2113(6)	0.2135(2)	Cu(1)—N(1)		0.2506(3)
N(1)—N(7)	0.2062(5)	0.20567(19)	Cu(1)—N(7)		0.2008(3)
N(1)—N(8)	0.2070(6)	0.2059(2)	Cu(1)—N(8)		0.2016(2)
Fe(1)—α(1)	0.1940(7)	0.1932(2)	Fe(1)—α(1)		0.1942(3)
Fe(1)—α(2)	0.1946(7)	0.1938(3)	Fe(1)—α(2)		0.1945(4)
Fe(1)—α(3)	0.1947(8)	0.1941(3)	Fe(1)—α(3)		0.1950(4)
Fe(1)—α(4)	0.1941(8)	0.1934(3)	Fe(1)—α(4)		0.1941(4)
Fe(1)—α(5)	0.1929(7)	0.1941(3)	Fe(1)—α(5)		0.1941(4)
Fe(1)—N(6)	0.1649(7)	0.1662(2)	Fe(1)—N(6)		0.1660(3)
α(1)—N(6)	0.1139(8)	0.1126(3)	α(1)—N(6)		0.1133(4)
N(1)—α(1)	0.1131(8)	0.1143(3)	N(1)—α(1)		0.1141(4)
α(1)—N(1)—N(1)	172.6(6)	152.57(19)	α(1)—N(1)—Cu(1)		136.37
N(7)—N(1)—N(8)	85.4(2)	85.52(8)	N(7)—Cu(1)—N(8)		86.10(10)
N(7)—N(1)—N(1)	88.5(2)	92.85(8)	N(7)—Cu(1)—N(1)		88.10(10)
N(8)—N(1)—N(1)	90.9(2)	89.04(8)	N(8)—Cu(1)—N(1)		91.82(10)
N(6)—Fe(1)—α(1)	96.2(3)	95.49(10)	N(1)—α(1)—Fe(1)		179.5(3)
N(6)—Fe(1)—α(2)	97.7(3)	96.90(12)	N(2)—α(2)—Fe(1)		176.7(4)
N(6)—Fe(1)—α(3)	176.8(3)	177.53(12)	N(3)—α(3)—Fe(1)		176.6(3)
N(6)—Fe(1)—α(4)	94.8(3)	93.26(11)	N(4)—α(4)—Fe(1)		175.9(3)
N(6)—Fe(1)—α(5)	91.5(3)	96.19(11)	N(5)—α(5)—Fe(1)		176.9(3)
α(1)—N(6)—Fe(1)	175.5(6)	179.0(2)	α(1)—N(6)—Fe(1)		179.4(3)
N(1)—α(1)—Fe(1)	174.4(7)	174.9(2)	N(6)—Fe(1)—α(1)		93.28(13)
N(2)—α(2)—Fe(1)	176.5(7)	177.3(3)	N(6)—Fe(1)—α(2)		96.81(15)
N(3)—α(3)—Fe(1)	176.4(7)	175.6(3)	N(6)—Fe(1)—α(3)		178.20(15)
N(4)—α(4)—Fe(1)	177.9(7)	176.0(3)	N(6)—Fe(1)—α(4)		93.48(14)
N(5)—α(5)—Fe(1)	179.1(7)	177.2(2)	N(6)—Fe(1)—α(5)		96.82(14)

As usual, the $[\text{Fe}(\text{CN})_5(\text{NO})]^-$ moiety exhibits a distorted octahedral structure, with the mean Fe—C, Fe—N, N—O and C—N bond lengths of 0.1941, 0.1649, 0.1145 and 0.1139 nm, respectively. The Fe—C—N and Fe—N—O bond angles range from 174.4° to 179.1° . These values are in good agreement with those in the previous reports.^{6,10}

As shown in the unit cell plot (Fig. 2) of complex **1**, all the NiFe_2 units align in the same direction and are parallel to each other to form a well-arranged ordered structure.

The molecules are connected by N—H...N and N—H...O hydrogen bonds leading to a 3D network. The N(10) atom of the NH_3^+ group and the N(8) atom coordinated with the Ni center are involved in the N—H...O_{water} hydrogen bonds with the N...O distances ranging from 0.2825 to 0.3136 nm. The N(5) atom of the $[\text{Fe}(\text{CN})_5(\text{NO})]^-$ anion and the N(7) atom in the macrocyclic ligand are connected by the hydrogen bond with N...N distance of 0.3029 nm and N—H...N angle of 146.67° .

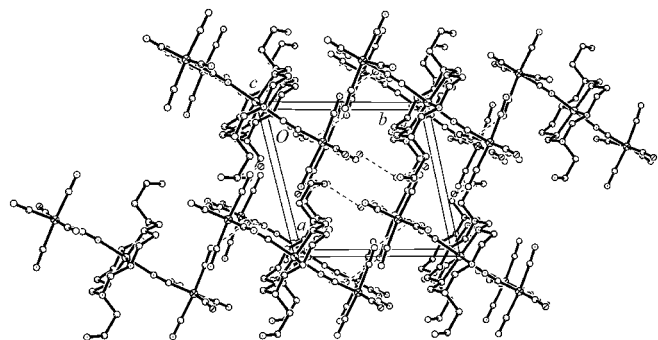


Fig. 2 Unit cell packing diagram of **1**. Hydrogen bonds are indicated by broken lines.

Fig. 3 shows the ORTEP plot of complex **2**. The crystal structure of complex **2** is similar to that of complex **1** with the difference in the number of free H_2O molecules and the bond distances and angles. The $\text{C}(1)\text{—N}(1)\text{—N}(1)$ bond angle of $152.57(19)^\circ$ is obviously smaller than that of complex **1**, but in accordance with that in other analogs.

Complexes **1** and **2** belong to the different space groups $P1$ and $P2_1/n$, respectively, which indicates that they have different packing modes (Fig. 4). The spatial configuration of complex **2** can be described as interlaced 2D layers. All the NiFe_2 units of the same layer are parallel but not parallel to those of the adjacent two layers.

Complex **2** also forms a 3D network via hydrogen bonds, but the situations are different from that of complex **1**. The N(10) atom of NH_3^+ anion is not only connected with O(2)_{water} atom but also connected with N(4) and N(5) atoms of $[\text{Fe}(\text{CN})_5(\text{NO})]^-$ anion by hydrogen bonds. The N(7) and N(8) atoms of macrocyclic ligand are connected with N(3) atom of the nearby trinuclear molecule and the O(3)_{water} atom, respectively, via hydrogen bonds.

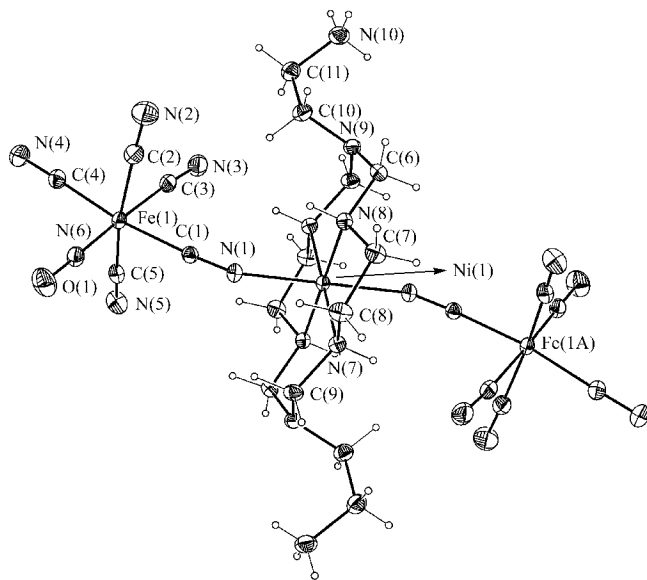


Fig. 3 ORTEP drawing of **2** with atomic numbering scheme, showing thermal ellipsoids at the 30% probability level.

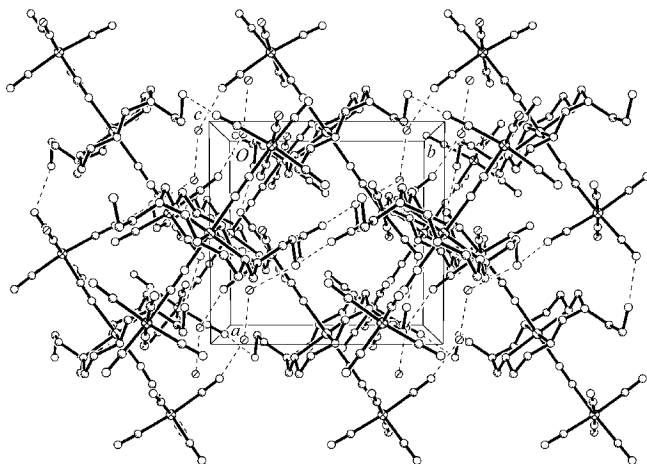


Fig. 4 Unit cell packing diagram of **2**. Hydrogen bonds are indicated by broken lines.

The ORTEP drawing of complex **3** is illustrated in Fig. 5. Complex **3** is isomorphous with complex **2**. The central Cu atom is also six-coordinated by N atoms leading to a distorted octahedron structure with four N atoms from the L ligand defining the equatorial plane and two N atoms from two bridging CN^- ligands occupying the axial positions. The Cu—N_{equatorial} bond lengths (ranging from 0.2008 to 0.2016 nm) is shorter than the Cu—N_{axial} bond lengths (0.2506 nm) due to the Jahn-Teller effect for the d^9 configuration of the Cu(II) ion in an octahedral environment. The bridging cyanides are coordinated to the Cu(II) ions in a bent fashion with the $\text{C}(1)\text{—N}(1)\text{—Cu}(1)$ bond angle of 136.37° , which is similar to that of $\text{Cu}(\text{en})_2\text{Fe}(\text{CN})_5(\text{NO})$.⁷ The mean bond lengths and angles of $[\text{Fe}(\text{CN})_5(\text{NO})]^-$ anion are in accordance with the corresponding values in complexes **1** and **2** (Table 1).

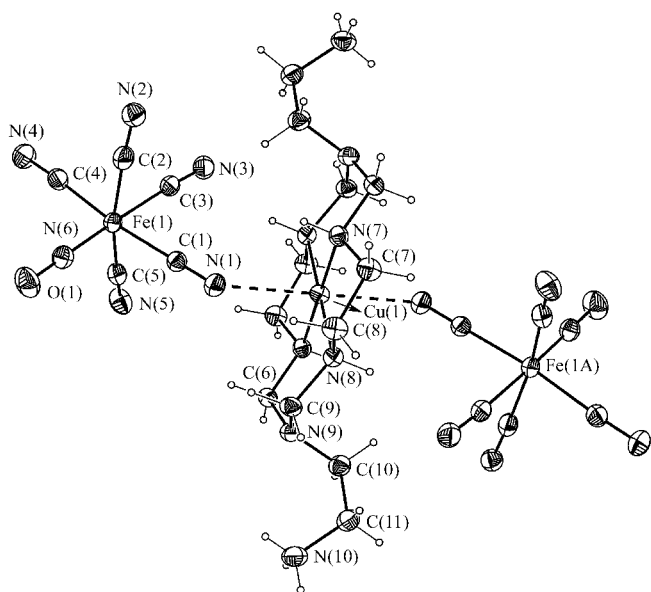


Fig. 5 ORTEP drawing of **3** with atomic numbering scheme, showing thermal ellipsoids at the 30% probability level.

The packing mode and the hydrogen bonds of complex **3** is almost the same as that of complex **2**, except some slight difference in bond lengths and angles.

Spectroscopic properties

Generally, IR absorption bands in the region 2200 – 1900 cm^{-1} are due to the $C\equiv N$ and $N=O$ stretching vibrations. Complexes **1**, **2** and **3** show strong band at 1937 , 1947 and 1924 cm^{-1} , respectively, which is reasonably assigned to the NO^+ stretching vibration. Strong bands at 2145 , 2146 and 2144 cm^{-1} which indicates the stretching vibration of terminal CN^- are observed for complexes **1**, **2** and **3**, respectively. Since the formation of the cyano bridge shifts $\nu(CN)$ towards higher frequency, the peaks at 2176 and 2169 cm^{-1} for complexes **1** and **2**, respectively, strongly demonstrate the presence of cyano bridges. There is no obvious peak observed at *ca.* 2170 cm^{-1} in complex **3**, which may be due to the weakness of interaction between CN^- and $Cu(II)$.

UV-vis spectra of **1** and **2** in aqueous solution are identical and exhibit a strong absorption with the λ_{max} at 200 nm ($\epsilon = 1500\text{ mol}^{-1}\cdot\text{L}\cdot\text{cm}^{-1}$) and a shoulder at 255 nm ($\epsilon = 20\text{ mol}^{-1}\cdot\text{L}\cdot\text{cm}^{-1}$), which are assigned to the ligand-to-metal charge transfer transition of $[Fe(CN)_5(NO)]^{3-}$. Very weak signals near 400 nm can be due to the d-d transitions of the $Ni(II)$ ions. UV-vis spectrum of **3** in aqueous solution exhibits a weak asymmetrical broad absorption with the λ_{max} at 514 nm ($\epsilon = 1.5\text{ mol}^{-1}\cdot\text{L}\cdot\text{cm}^{-1}$), which is assigned to d-d transition of the $Cu(II)$ ions. Compared with the UV-vis spectrum of the $Cu(II)$ precursor,¹⁴ substitution of isocyano- for perchlorato-ligand shifts the band by 12 nm towards higher frequencies, as would be expected from spectrochemical considerations.

Considering that the nitroprusside group is diamagnet-

ic, the electron paramagnetic resonance (EPR) spectra of **3** may provide some useful information about the electronic structure of the $Cu(II)$ ion. The powder X-band EPR spectrum measured at room temperature showing hyperfine splitting around the $g_{//}$ region is typical of an isolated d^9 complex (Fig. 6). Analysis of the spectrum affords parameters of $g_{//} = 2.19$ and $A_{//} = 200\text{ G}$, which are in good agreement with those for mononuclear copper(II) compounds.^{14,15} The spectrum is very similar to that for the precursor $[Cu(H_2L)](ClO_4)_4$.¹⁴ This is understandable considering that both complexes possess similar $Cu(II)$ coordination surroundings (CuN_6 for **3** and CuN_4O_2 for $[Cu(H_2L)](ClO_4)_4$). The EPR spectrum in an aqueous solution exhibits four isotropic hyperfine peaks with the parameters of $a_{iso} = 90\text{ G}$ and $g_{iso} = 2.10$.

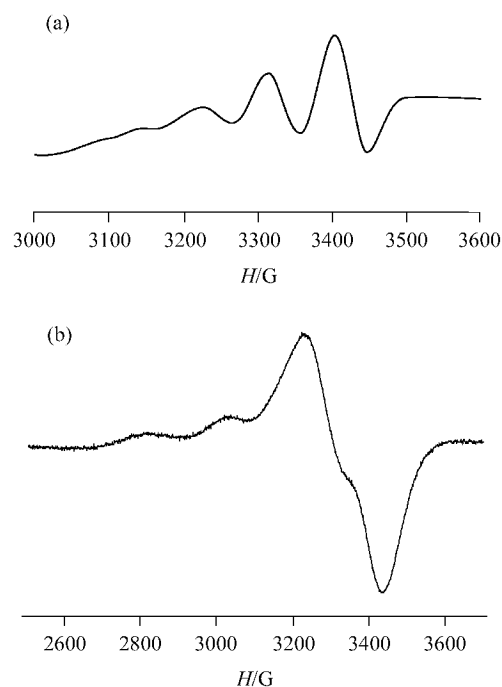


Fig. 6 EPR spectra of **3** recorded at room temperature: (a) aqueous solution, (b) solid.

In conclusion, the results showed that new cyano-bridged trinuclear species could be generated via the control of the charge of the building blocks. It can be therefore anticipated that other trinuclear NiM_2 containing paramagnetic ($[Ni(CN)_5]^{3-}$ or $[Fe(CN)_5]^{3-}$) and hexavalent $[Ni^{II}H_4L]^{3+}$ precursors could be prepared. Further work along this line is in progress in our laboratory.

Experimental

Elemental analyses of carbon, hydrogen, and nitrogen were carried out with an Elementar Vario EL. The infrared spectroscopy was performed on a Magna-IR 750 spectrophotometer in the 4000 – 400 cm^{-1} region. The electronic spectra of **1**–**3** were measured with a Perkin Elmer Hitachi-240 spectrophotometer in water. The room-temper-

ature EPR spectra of **3** were recorded at X-band with a Bruker ER 200B spectrometer.

[Cu(H₂L)] [ClO₄]₄ and [Ni(H₂L)] [ClO₄]₄ were prepared by the reported method.^{14,16} [Ni(H₂L)] Br₄ is prepared by a method similar to [Ni(H₂L)] [ClO₄]₄ except employing HBr to take the place of HClO₄.

Complex 1 Slow evaporation of the aqueous solution of [Ni(H₂L)] [ClO₄]₄ and Na₂[Fe(CN)₅(NO)] · 2H₂O (molar ratio , 1 : 1) at room temperature resulted in the light brown crystals suitable for single crystal analysis. UV-vis (H₂O) λ_{max} : 200 , 255 , 400 nm ; IR ν : 2169 , 2146 , 1947 cm⁻¹. Anal. calcd for NiFe₂C₂₂N₂₀H₄₆O₈ : C 29.72 , H 5.21 , N 31.51 ; found C 29.57 , H 5.10 , N 31.46.

Complex 2 Light brown single crystals were formed by slow evaporation of [Ni(H₂L)] Br₄ and Na₂[Fe(CN)₅(NO)] · 2H₂O (molar ratio , 1 : 1) in water at room temperature. UV-vis (H₂O) λ_{max} : 200 , 255 , 400 nm ; IR ν : 2176 , 2145 , 1937 cm⁻¹. Anal. calcd for NiFe₂C₂₂H₄₂N₂₀O₆ : C 30.97 , H 4.96 , N 32.84 ; found C 31.98 , H 4.67 , N 33.38.

Complex 3 The same method for the preparation of complex **1** was adopted except the replacement of [Ni-

(H₂L)] [ClO₄]₄ by [Cu(H₂L)] [ClO₄]₄, and red crystals were obtained. UV-vis (H₂O) λ_{max} : 514 nm ; IR ν : 2144 , 1924 cm⁻¹. Anal. calcd for CuFe₂C₂₂N₂₀H₄₂O₆ : C 30.46 , H 4.95 , N 32.65 ; found C 30.80 , H 4.95 , N 32.07.

Crystallographic data collection and structure determination

Crystal data of complexes **1** , **2** and **3** were collected on a Rigaku R-Axis RIPID IP , a Bruker Smart CCD and a Bruker P4 diffractometer , respectively , with graphite-monochromated Mo Kα radiation. Intensity data were corrected for Lp effects and φ absorption correction. The structures were solved by direct method (SHELXS-97¹⁷) and refined by full-matrix least-squares (SHELXL-97¹⁸) on F². Hydrogen atoms were added geometrically and refined using a riding model. Crystal data of complexes **1** , **2** and **3** are presented in Table 2. CCDC-196870-196872 contains the supplementary crystallographic data for this paper. These data can be obtained free of charge via www.ccdc.cam.ac.uk/conts/retrieving.html (or from the Cambridge crystallographic Data Centre , 12 , Union Road , Cambridge CB2 1EZ , UK ; Fax : (+ 44) 1223-336-033 ; or deposit@ccdc.cam.ac.uk).

Table 2 Crystal data for **1** , **2** and **3**

Crystal data	1	2	3
Empirical formula	NiFe ₂ C ₂₂ H ₄₆ N ₂₀ O ₈	NiFe ₂ C ₂₂ H ₄₂ N ₂₀ O ₆	CuFe ₂ C ₂₂ H ₄₂ N ₂₀ O ₆
Formula weight	889.2	853.17	858
Temperature (K)	123(2)	293(2)	293(2)
Measurement device	Rigaku R-Axis RIPID IP	Bruker Smart CCD	Bruker P4
Wavelength (nm)	0.071073	0.071073	0.071073
Crystal system	Triclinic	Monoclinic	Monoclinic
Space group	$P\bar{1}$	$P2_1/n$	$P2_1/n$
<i>a</i> (nm)	1.0464(2)	1.0354(2)	1.0499(2)
<i>b</i> (nm)	1.0581(2)	1.0828(2)	1.0996(2)
<i>c</i> (nm)	0.9788(2)	1.6292(3)	1.5839(3)
α (°)	95.02(3)		
β (°)	76.12(3)	96.06(3)	94.39(12)
γ (°)	109.03(3)		
Volume (nm ³)	0.9945(3)	1.8163(6)	1.8233(6)
<i>Z</i>	1	2	2
<i>D</i> _c (Mg/m ³)	1.485	1.56	1.563
<i>F</i> (000)	462	884	886
μ (mm ⁻¹)	1.225	1.367	1.429
Reflections collected/unique	3922/3922	16784/6677	4187/3203
Reflections with <i>I</i> > 2σ(<i>I</i>)	1836	5022	2755
Goodness-of-fit on <i>F</i> ²	0.894	1.025	0.973
<i>R</i> ₁ [<i>I</i> > 2σ(<i>I</i>)]	0.0704	0.0535	0.0388
<i>wR</i> ₂ (all data)	0.1489	0.1485	0.0829

References

- 1 Playfair, L. *Proc. R. Soc. London* **1848**, *5*, 846.
- 2 Kalecinska, E.; Jesowaka-Trzebiatowska, B. *Radiochem. Radioanal. Lett.* **1980**, *44*, 17.
- 3 Narbutt, J.; Siwinski, J.; Bartos, B.; Bilewicz, A. *J. Radioanal. Nucl. Chem.* **1986**, *101*, 41.
- 4 Mullica, D. F.; Hayward, P. K.; Sappenfield, B. L. *Inorg. Chim. Acta* **1995**, *237*, 111.
- 5 Misra, H. P. *J. Biol. Chem.* **1984**, *259*, 12678.
- 6 Shyu, H. L.; Wei, H. H.; Wang, Y. *Inorg. Chim. Acta* **1997**, *258*, 81.
- 7 Kou, H.-Z.; Wang, H.-M.; Liao, D.-Z.; Cheng, P.; Jiang, Z.-H.; Yan, S.-P.; Huang, X. Z.; Wang, G.-L. *Aust. J. Chem.* **1998**, *51*, 661.
- 8 Zhang, K. L.; Xu, Y.; Wang, Z.; Jin, C. M.; You, X. Z. *Transition Met. Chem.* **2002**, *27*, 95.
- 9 Chen, Z. N.; Wang, J. L.; Qiu, J.; Miao, F. M.; Tang, W. X. *Inorg. Chem.* **1995**, *34*, 2255.
- 10 Mondal, N.; Saha, M. K.; Mitra, S.; Gramlich, V.; Falah, M. S. E. *Polyhedron* **2000**, *19*, 1935.
- 11 Smekal, Z.; Travnicek, Z.; Marek, J.; Nadvornik, M. *Aust. J. Chem.* **2000**, *53*, 225.
- 12 Zhang, H.; Cai, J. W.; Feng, X.-L.; Sang, H.-Y.; Liu, J.-Z.; Li, X.-Y.; Ji, L.-N. *Polyhedron* **2002**, *21*, 721.
- 13 Kou, H.-Z.; Zhou, B. C.; Liao, D.-Z.; Wang, R.-J.; Li, Y. D. *Inorg. Chem.* **2002**, *41*, 6887.
- 14 He, Y.; Kou, H.-Z.; Li, Y.; Zhou, B. C.; Xiong, M.; Li, Y. D. *Inorg. Chem. Commun.* **2003**, *6*, 38.
- 15 Li, Z.-Y.; Xu, D.-J.; Shi, W.-L.; Chen, D.-Y.; Wu, J.-Y.; Chiang, M. Y. *Chin. J. Chem.* **2002**, *20*, 390.
- 16 Kang, S. G.; Ryu, K.; Jung, S. K.; Kim, J. *Inorg. Chim. Acta* **1999**, *293*, 140.
- 17 Sheldrick, G. M. *SHELXS 97, Program for Crystal Structure Solution*, University of Göttingen, Germany, **1997**.
- 18 Sheldrick, G. M. *SHELXL 97, Program for Crystal Structure Refinement*, University of Göttingen, Germany, **1997**.

(E0303171 PAN, B. F.; FAN, Y. Y.)